Cell, Vol. 102, 521–531, August 18, 2000, Copyright ©2000 by Cell Press

# Hedgehog Induces Opposite Changes in Turnover and Subcellular Localization of Patched and Smoothened

**Natalie Denef, Dagmar Neubüser, Lidia Perez, and Stephen M. Cohen***
European Molecular Biology Laboratory
Meyerhofstr 1
69117 Heidelberg
Germany

## Summary

**Secreted signaling proteins of the Hedgehog family organize spatial pattern during animal development. Two integral membrane proteins have been identified with distinct roles in Hedgehog signaling. Patched functions in Hedgehog binding, and Smoothened functions in transducing the signal. Current models view Patched and Smoothened as a preformed receptor complex that is activated by Hedgehog binding. Here we present evidence that Patched destabilizes Smoothened in the absence of Hedgehog. Hedgehog binding causes removal of Patched from the cell surface. In contrast, Hedgehog causes phosphorylation, stabilization, and accumulation of Smoothened at the cell surface. Comparable effects can be produced by removing Patched from cells by RNA-mediated interference. These findings raise the possibility that Patched acts indirectly to regulate Smoothened activity.**

## Introduction

Signaling proteins of the Hedgehog (Hh) family transmit information between cell populations to organize spatial pattern during development. In *Drosophila*, Hh signaling organizes long-range and short-range pattern in the wings and legs (Basler and Struhl, 1994; Diaz-Benjumea et al., 1994; Tabata and Kornberg, 1994; Zecca et al., 1995). Hh acts directly to regulate growth and patterning of the central region of the wing (Mullor et al., 1997; Strigini and Cohen, 1997). In addition, Hh signaling induces localized expression of the secreted signaling proteins Wingless and Decapentaplegic, which act at long range to organize the anteroposterior axis of the wing and the dorsoventral and proximodistal axes of the leg (Brook and Cohen, 1996; Jiang and Struhl, 1996; Lecuit et al., 1996; Nellen et al., 1996; Lecuit and Cohen, 1997).

The ability of Hh to convey positional information in the developing limbs is based on asymmetry in the properties of cells sending and receiving the Hh signal. Several components of the Hh pathway are differentially expressed in anterior (A) and posterior (P) cells, including the Hh binding receptor Patched (Ptc) and the zinc finger transcription factor Cubitus interruptus (Ci). Posterior cells express Hh (Lee et al., 1992; Tabata et al., 1992) but are not responsive to it because they lack Ci (Motzny and Holmgren, 1995; Schwartz et al., 1995; Dominguez et al., 1996; Hepker et al., 1997; Aza-Blanc and Kornberg, 1999). Hh signaling controls Ci activity by reducing production of the repressor form of Ci and stimulating production and nuclear translocation of the activator form of Ci (Aza-Blanc et al., 1997; Ohlmeyer and Kalderon, 1998; Chen et al., 1999; Méthot and Basler, 1999; Wang and Holmgren, 1999). By this means, Hh signaling induces transcriptional activation of a number of Ci-dependent target genes, including the Hh receptor Ptc (Alexandre et al., 1996). Ptc is expressed throughout the A compartment and is upregulated by Hh signaling in cells close to the AP boundary, where it binds Hh and limits its movement into the A compartment (Chen and Struhl, 1996). Thus, Hh limits its own range of movement by controlling expression of its receptor.

Hh signaling requires the activity of two transmembrane proteins. Ptc is a multipass membrane protein that serves as the Hh binding receptor (Marigo et al., 1996; Stone et al., 1996). Smoothened is a seven-pass membrane protein that is required to transduce the signal (Alcedo et al., 1996; Chen and Struhl, 1996, 1998; van den Heuvel and Ingham, 1996). Genetic analysis has shown that Ptc activity antagonizes Hh signaling by blocking the intrinsic signaling activity of Smoothened (Ingham et al., 1991; Alcedo et al., 1996; Chen and Struhl, 1996). The mechanism by which Ptc regulates Smoothened is not understood, but the observation that the two proteins were coimmunoprecipitated from transfected cells has led to the idea that Ptc and Smoothened are present in a preformed complex that is activated by Hh binding (Stone et al., 1996). One interpretation of these results is that Hh binding might induce a conformational change in the preformed Patched–Smoothened complex that alleviates Ptc-mediated repression of Smoothened activity (Stone et al., 1996; Alcedo and Noll, 1997; Chen and Struhl, 1998). Evidence is presented here in support of a different model. Hedgehog binding causes internalization of Ptc from the cell surface while at the same time promoting accumulation of Smoothened at the cell surface. Hh binding to Ptc induces phosphorylation of Smoothened. Comparable results were obtained by depletion of Ptc by RNA-mediated interference. We propose that Ptc acts indirectly to regulate Smoothened perhaps by promoting activity of a phosphatase that dephosphorylates Smoothened in the absence of Hh activity.

## Results

### Differential Expression of Smoothened in A and P Compartments

As a first step toward addressing how Smoothened activity is regulated by Ptc, we produced an antibody to the C-terminal cytoplasmic tail of Smoothened (Smo) protein and examined Smo expression in imaginal discs. Ptc and Smo are both differentially expressed in A and P cells but in different ways. Ptc is absent from P cells, whereas Smo is expressed at relatively high levels in the P compartment (Figures 1A–1C). In the A compartment, Smo levels follow a profile similar to Ptc. Smo protein

*To whom correspondence should be addressed (e-mail: cohen@embl-heidelberg.de).

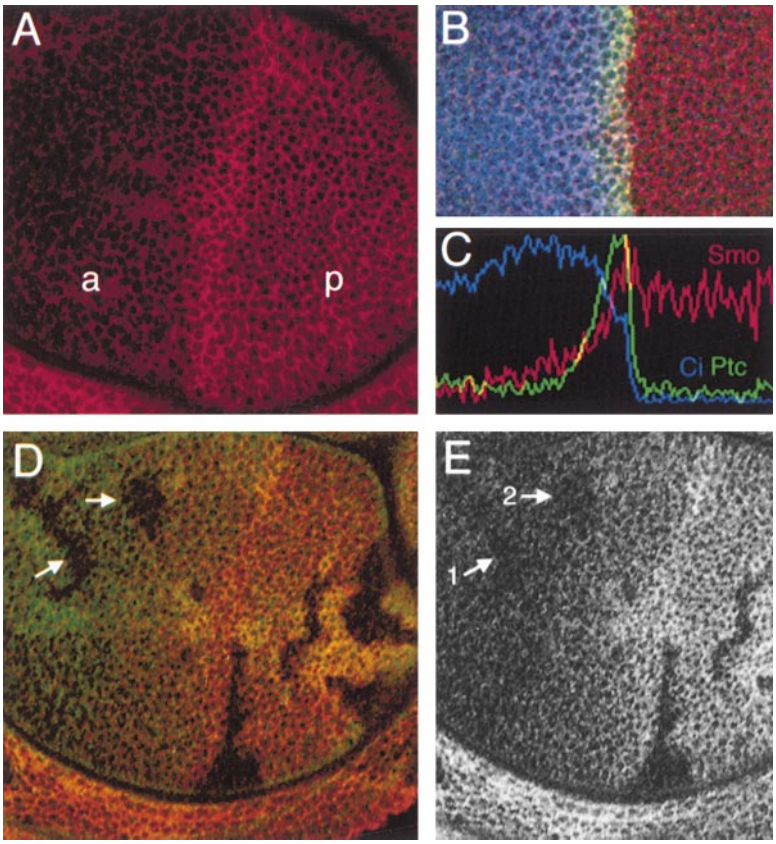


Figure 1. Smo Expression

(A) Wing imaginal disc labeled for Smo protein (red). Smo protein is distributed unequally across the wing pouch. Higher levels can be detected in the posterior compartment (p) than in the anterior compartment (a). Highest Smo levels occur in anterior cells adjacent to the AP compartment boundary. Smo expression also differs between a and p compartments in leg discs, except that local induction immediately adjacent to the AP boundary is less pronounced in the leg (data not shown). In this and all subsequent figures, wing discs are shown with anterior to the left and dorsal up.

(B) Detail of the central two-thirds of the wing pouch of a disc labeled for Smo (red), Ptc (green), and Ci (blue).

(C) Quantitation of expression levels of the image in (B). Smo levels decrease sharply in cells close to the AP boundary and then more slowly across the anterior compartment. Ptc and Ci mark anterior cells. Range of intensity values (scale = 0–256): Smo, 16–57; Ptc, 20–67; Ci, 5–72.

(D and E) Wing disc with several clones of cells mutant for *smo*$^{3}$. Clones are marked with the absence of β-galactosidase protein (green). Smo protein is shown in red. Smo staining is absent from the clones. (E) Smo expression shown separately.

levels are highest in Hh-responsive anterior cells adjacent to the AP boundary (Figures 1A–1C). Smo expression decreases sharply near the boundary and then more gradually across the A compartment (Figure 1C). To verify that this accurately reflects Smo protein levels, we examined clones of cells mutant for the *smo*$^{3}$ allele (Figures 1D and 1E). *smo*$^{3}$ is associated with a nonsense mutation that truncates the protein after the third transmembrane domain (Chen and Struhl, 1998). The C-terminal intracellular portion of the protein recognized by anti-Smo should be absent from the protein encoded by this allele. Clones of mutant cells in both compartments lacked Smo antigen (Figures 1D and 1E). Smo protein was clearly detectable in cells adjacent to the mutant clone in the middle of the A compartment (Figure 1E, clone 2). The level of Smo in wild-type cells adjacent to a more anterior clone was barely distinguishable from background (Figure 1E, clone 1).

Although Smo protein expression levels differ in the A and P compartments, *smo* mRNA does not appear to be spatially regulated in the wing or leg imaginal discs. In situ hybridization using sense and anti-sense RNA probes did not detect differential expression of *smo* mRNA in A and P compartments of the wing disc (Figures 2A and 2B) or of the leg disc (data not shown). *smo* transcript is expressed in a spatially regulated pattern in the brain (Figures 2C and 2D), which corresponds to the pattern of Smo protein expression (Figure 2E).

### Posttranscriptional Regulation of Smo Protein Levels

The observation that *smo* mRNA and protein distributions do not correspond in the imaginal discs suggested that Smo might be regulated posttranscriptionally in the discs. To test this, we expressed *smo* mRNA under control of heterologous promoters that are not subject to spatial regulation along the AP axis of the wing disc. Clones of cells expressing *smo* mRNA were produced using a flip-out construct expressing GAL4 under control of the actin promoter. Clones were marked by coexpression of GFP and Smo. GFP levels were comparable in A and P clones (Figure 2F, green arrows), but Smo levels were much lower in A clones (Figure 2F, red arrows). Comparable results were obtained when an epitope-tagged version of Smo was expressed in the dorsal compartment of the disc under *apterous*$^{GAL4}$ control. Smo expression was visualized using anti-Smo and an antibody that binds to the epitope tag. Both antibodies detected higher levels of Smo in the P compartment (Figure 2G). For comparison, the level of endogenous Smo in P cells can be seen faintly in ventral cells that do not express *apterous*$^{GAL4}$. Use of the epitope tag to visualize Smo protein excludes the possibility that superimposition of endogenous and overexpressed Smo might contribute to the appearance of differential expression in A and P cells. Comparable AP differences in Smo levels were seen in the leg disc (data not shown). We conclude that Smo is regulated posttranscriptionally in the imaginal discs.

### Hh-Dependent and Hh-Independent Regulation of Smo

The observation that Smo levels are highest in A cells adjacent to the AP boundary suggested a role for Hh signaling in regulation of Smo levels. To test whether

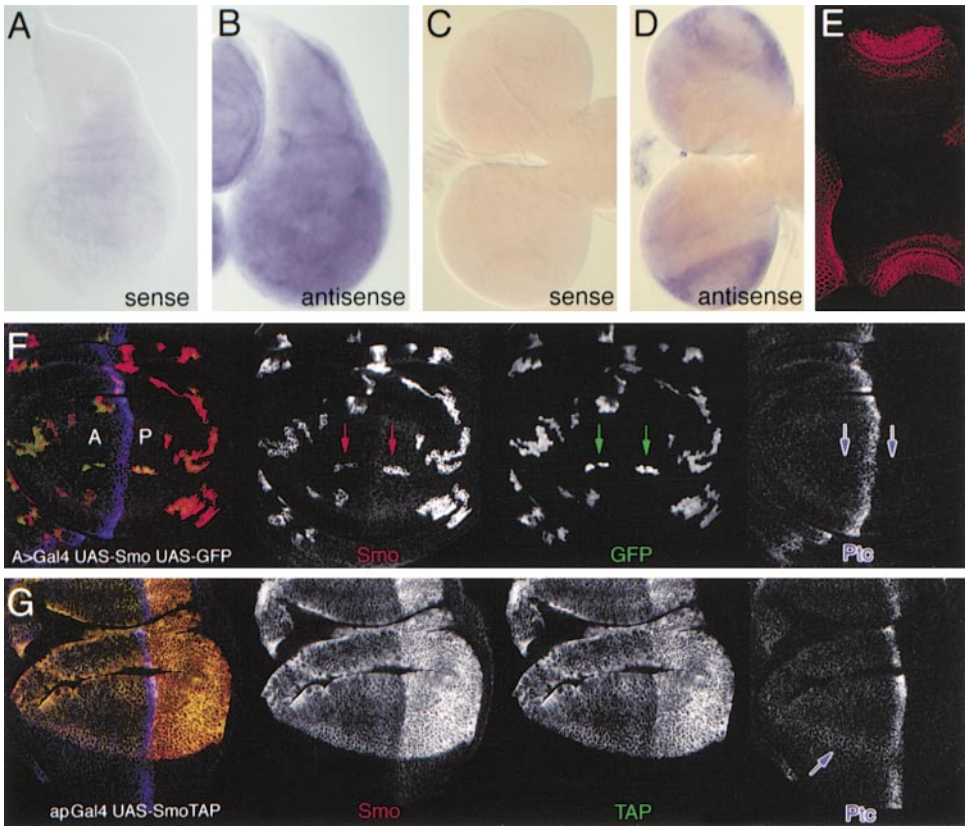


Figure 2. Posttranscriptional Regulation of Smo

(A and B) In situ hybridization of wing discs with *smo* RNA probes: (A) sense probe, (B) antisense probe. *smo* mRNA levels do not differ between A and P compartments in the wing disc. Comparable results were obtained in leg discs (data not shown).

(C and D) In situ hybridization of third instar larval brains with *smo* RNA probes: (C) sense probe, (D) antisense probe. Note localized Smo expression in the brain.

(E) Smo protein is expressed in a corresponding pattern. The labeling at lower left is part of an eye disc.

(F) Wing disc with multiple clones of cells expressing Smo under GAL4 control (*act5c>stop>GAL4/HS-Flp; UAS-Smo/+; UAS-GFP/+*). Left panel: Smo protein is shown in red. Clones are marked by coexpression of GFP (green). Ptc protein is shown in blue to mark the AP boundary. Smo, GFP, and Ptc channels are shown separately at right. Smo protein levels are lower in A clones compared to P clones (e.g., red arrows), while GFP protein levels are similar in both compartments (e.g., green arrows). Note that the level of GAL4-dependent Smo expression is much higher than the endogenous Smo level, which is only faintly visible in the P compartment. Ptc expression was not induced in A clones overexpressing Smo.

(G) Expression of an epitope-tagged version of Smo (Smo-TAP) in the dorsal compartment under *apterous*$^{GAL4}$ control. Smo protein is shown in red. The TAP tag is shown in green. Ptc is shown in blue to mark the AP boundary. The three channels are shown separately at right. Smo-TAP levels are higher in P than in A cells. This difference can be detected with an antibody bound by the TAP tag that eliminates the possibility that the difference detected in overexpressed protein is simply a superposition of differentially distributed endogenous protein and homogeneously overexpressed protein. Overexpression of Smo-TAP under *apterous*$^{GAL4}$ control causes a slight induction of Ptc in dorsal cells (arrow, right panel).

Hh is capable of inducing Smo in A cells, clones of Hh-expressing cells were generated at random positions. Hh-expressing clones were marked by coexpression of GFP and examined for Smo and Ptc expression. The level of Smo protein was elevated in A cells expressing Hh and in nearby wild-type cells in which Ptc was also upregulated (Figure 3A). To verify that the elevated level of Smo in A cells is Hh dependent, we made use of the temperature-sensitive allele *hh*$^{ts2}$. *hh*$^{ts2}$ larvae were raised at 18°C until mid third instar and shifted to 29°C to inactivate Hh for the last 24 hr of larval development. Under these conditions, Hh-dependent transcription of *dpp*, *ptc* and anterior *en* as well as Hh-dependent post-translational regulation of Ci are completely abolished (Strigini and Cohen, 1997). As expected, removing Hh activity eliminated the local increase in Smo levels in Hh-responsive A cells so that Smo levels were uniformly low in A cells (Figure 3B). Comparable results were obtained when larvae were incubated at 29°C for the last 2 days of larval development. Intriguingly, Smo levels remained high in P cells in the absence of Hh activity. This observation reveals the existence of a mechanism to regulate Smo protein levels in a compartment-specific manner that does not depend directly on Hh activity.

### Ptc-Dependent Downregulation of Smo

As noted above, Ptc is expressed in A cells but not in P cells. To ask whether Ptc activity is responsible for the Hh-independent regulation of Smo levels, we examined the effects of *ptc* mutant clones on Smo expression. *ptc* mutant cells showed an autonomous increase in the

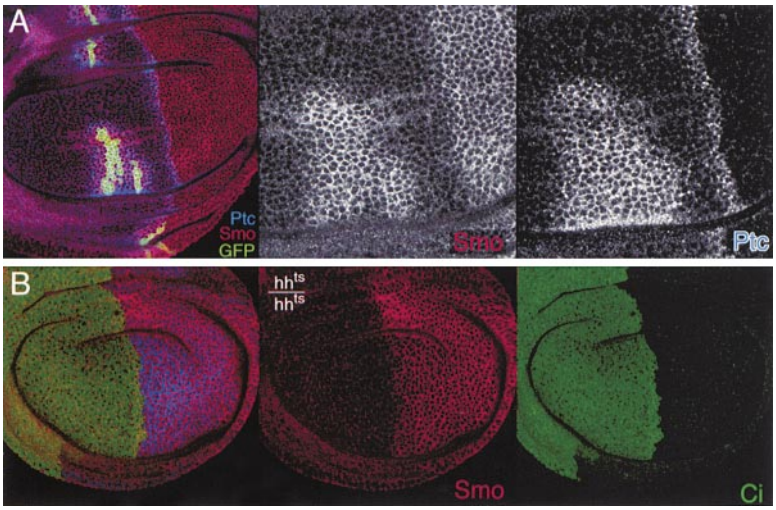


Figure 3. Hh-Dependent and Hh-Independent Regulation of Smo

(A) Wing disc with Hh-expressing clones. Smo is shown in red. Ptc is shown in blue. Clones are marked by coexpression of GFP (green). Higher magnification views of Smo and Ptc expression in the region around the clones are shown separately at right. Smo and Ptc protein levels are increased in the Hh-expressing cells and in nearby cells. Elevated Ptc is detected in cells at a greater distance from the clone than Smo. Ptc and Smo were induced cell autonomously by Hh-CD2-expressing clones (data not shown), indicating that Smo is directly upregulated by Hh and not by relay of a secondary signal.

(B) $hh^{ts2}$ homozygous mutant wing disc incubated for 24 hr at 29°C to inactivate Hh protein and labeled to visualize Ci (green), Smo (red), and Engrailed (blue). Smo expression was uniformly low in A cells but remained at elevated levels in P cells. Smo was not elevated in A cells adjacent to the AP boundary. Note that elevated Smo and Ci do not overlap. Loss of Hh activity was confirmed by the absence of Hh-dependent anterior En expression and by the irregular interface between A and P cells reflected by Ci labeling.

level of Smo protein (Figure 4A). This observation would be consistent with a role for Ptc in modifying Smo levels; however, interpretation of *ptc* clones is complicated by the fact that removing Ptc activity from A cells mimics Hh signaling (Ingham et al., 1991; Capdevila et al., 1994; Li et al., 1995; Chen and Struhl, 1996). Hh signaling involves stabilization of the activator form of Ci and its translocation to the nucleus (Aza-Blanc et al., 1997; Ohlmeyer and Kalderon, 1998; Chen et al., 1999; Méthot and Basler, 1999; Wang and Holmgren, 1999). Ci stabilization occurs in Ptc clones, leading to expression of Hh target genes. Ectopic expression of Ci in the P compartment can induce elevated levels of Smo protein (data not shown). Consequently, we cannot distinguish whether the increase in Smo in *ptc* mutant clones is due to the absence of Ptc per se or due to Ci-dependent induction of Smo in A cells. To ask whether Smo levels are elevated as a consequence of removing Ptc protein, we examined the effects of expressing Ptc in the P compartment where Hh targets cannot be activated due to the absence of Ci. When Hh was active, Ptc-expressing clones had little or no effect on Smo protein levels

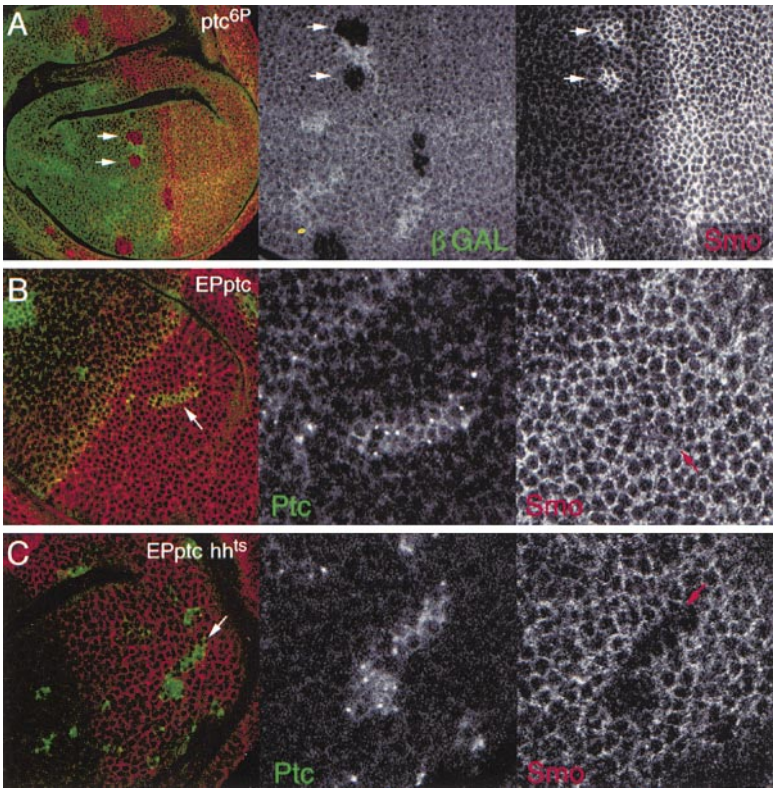


Figure 4. Ptc Downregulates Smo in the Absence of Hh

(A) Wing disc with several clones of cells mutant for $ptc^{6P}$. Clones are marked by the absence of β-galactosidase (green). Smo protein (red) is upregulated in the clones. Magnified view of β-gal and Smo expression are shown separately in the middle and right panels. $ptc^{6P}$ is a strong allele that produces a nonfunctional Ptc protein. Comparable results were obtained with clones mutant for the protein null allele $ptc^{IIW}$.

(B and C) Wing discs with clones of cells expressing Ptc (green) and labeled for Smo (red). $hh^{ts2}/+$ heterozygous controls and $hh^{ts2}$ homozygous larvae were shifted to 29°C for the last 24 hr of development.

(B) $hh^{ts2}/+$ heterozygous disc. Smo levels are unaltered both in anterior and posterior Ptc-expressing clones. Magnified views of Ptc and Smo expression in a P compartment clone shown separately in the middle and right panels.

(C) $hh^{ts2}$ homozygous disc. Upregulation of Ptc and Smo does not occur in cells adjacent to the AP boundary due to inactivation of Hh. Magnified views of Ptc and Smo expression in a P clone are shown separately in the middle and right panels. Smo levels are reduced in posterior Ptc-expressing clones. No obvious changes were detected in anterior clones.

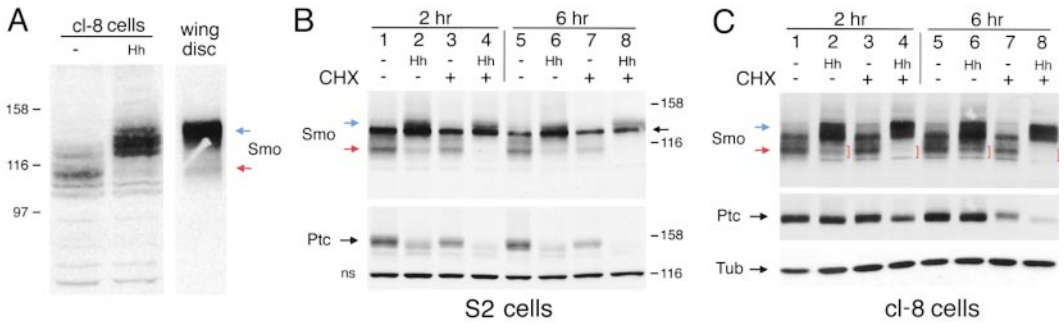


Figure 5. Posttranslational Regulation of Ptc and Smo

(A) Immunoblot of clone 8 cell and wing imaginal disc lysates probed with anti-Smo. Cells were treated for 6 hr with S2-conditioned medium (−) or with Hh-N-conditioned medium (Hh). The disc and cell lysates were run on the same gel (intervening lanes are not shown). The red arrow indicates Smo in the faster migrating form. The blue arrow indicates the more abundant slower migrating form in disc lysates.

(B) Immunoblots of Schneider S2 cell lysates probed with rat anti-Smo and subsequently reprobed with mouse anti-Ptc. Cells were treated with S2-conditioned medium (−) or with Hh-N-conditioned medium (Hh). CHX: plus sign indicates cycloheximide added to 10 μM. Minus sign indicates no cycloheximide added. Lanes 1–4 were treated for 2 hr. Lanes 5–8 were treated for 6 hr. Red and blue arrows indicate faster and slower migrating forms of Smo. The black arrow at right indicates an abundant protein that binds nonspecifically to anti-Smo in some preparations. "ns" indicates a background band detected in S2 cells with anti-Ptc. The level of ns protein does not change following cycloheximide or Hh treatment.

(C) Immunoblots of clone 8 cell lysates treated as in (A). The blot was probed with anti-Smo and subsequently with anti-Ptc and anti-tubulin.

in the P compartment (Figure 4B). In contrast, in the *hh*$^{ts2}$ mutant background, Ptc-expressing clones reduced Smo protein to a level comparable to that in A cells at a distance from the boundary (Figure 4C). The effect of Ptc was cell autonomous. These results indicate that Ptc activity is sufficient to reduce Smo levels in A cells in the absence of Hh. We suggest that the elevated level of Smo in P cells is the default state and that Ptc is responsible for the Hh-independent downregulation of Smo levels in A cells. Hh binding appears to prevent Ptc from doing so and further induces Smo levels near the AP boundary.

### Posttranslational Modification of Smo

To ask how Ptc and Hh regulate Smo levels, we turned to *Drosophila* Schneider S2 cells and the clone 8 imaginal disc cell line (cl-8). Both cell lines express endogenous Smo and Ptc proteins (Figure 5), which allowed us to analyze their regulation without overexpressing the proteins by transfection. Smo protein from cl-8 cell lysates resolved into several protein forms of different electrophoretic mobility in denaturing gels. Treatment of cl-8 cells with Hh-conditioned medium induced accumulation of Smo and increased the proportion of Smo in the slower migrating forms. The Hh-induced forms of Smo in cl-8 cells comigrated with the major form of Smo protein in wing imaginal disc lysates (Figure 5A, blue arrow). A small fraction of Smo from the wing disc was present in the faster migrating form (red arrow). Most of Smo protein in the disc comes from the P compartment where Ptc is absent or from the Hh-responsive region where Ptc cannot downregulate Smo (Figure 1A).

Schneider S2 cells are Hh responsive but lack Ci and should be unable to induce transcription of known Hh target genes (Therond et al., 1996; Aza-Blanc et al., 1997). Nonetheless, Hh treatment of S2 cells induced accumulation of the slower migrating forms of Smo (Figure 5B, lanes 1, 2 and 5, 6). This was also the case when S2 cells were treated with Hh and cycloheximide to block new protein synthesis (Figure 5B, lanes 3 and 4). In both S2 cells and cl-8 cells treated with cycloheximide and Hh, the proportion of Smo in the faster migrating form was reduced compared to cells treated with Hh alone (Figure 5C, red brackets, lanes 2 and 4). This difference was more pronounced after 6 hr treatment with cycloheximide and Hh (lanes 6 and 8) and appears to reflect net accumulation of the slower migrating form when no new Smo is made. Taken together, these observations indicate that Smo undergoes Hh-dependent posttranslational modification.

To ask whether removing Ptc activity would be sufficient to mimic the effects of Hh treatment on Smo in S2 cells, we depleted Ptc using double-stranded RNA interference (Hammond et al., 2000). S2 cells were transfected with double-stranded (ds) *ptc* RNA or with control dsRNA and examined by immunoblotting for Ptc and Smo proteins at intervals after transfection. Ptc levels were considerably reduced by 8 hr of recovery (Figure 6, upper panel, compare lanes 1 and 3). Ptc decreased further over the next 24 hr and then remained at a constant level (lanes 4–7). Depletion of Ptc caused accumulation of Smo in the slower migrating form between 20 and 32 hr of recovery from transfection (Figure 6, lower panel, lanes 3–7). The effect on Smo accumulation and mobility was comparable to that caused by Hh treatment but occurred more slowly. This presumably reflects the time required for Ptc protein levels to decrease after new synthesis is blocked by RNA(i). Although Ptc levels were reduced considerably by 8 hr after transfection, the remaining protein was presumably active. In contrast, Hh binding rapidly blocks Ptc activity (Figure 5 and see below). Treatment of cells with control dsRNA had little or no effect on Ptc or Smo levels (Figure 6, lanes 8–12). These observations indicate that Hh-dependent inactivation of Ptc causes a change in posttranslational modification of Smo.

To determine the type of posttranslational modification responsible for the Hh-induced shift in the electrophoretic mobility of Smo, cl-8 cell lysates were treated with enzymes that remove modifications from proteins. Treatment of cl-8 lysates with the endoglycosidase PNGaseF to remove N-linked oligosaccharide side

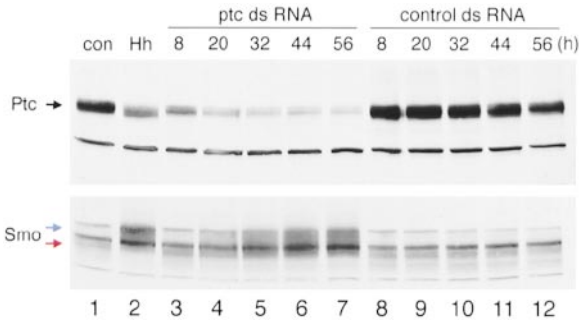


Figure 6. Depletion of Ptc Causes Smo Modification

Immunoblots of S2 cell lysates probed with rat anti-Smo (lower panel) and subsequently reprobed with mouse anti-Ptc (upper panel). Lanes 1 and 2: cells treated with S2 conditioned medium (con) or with Hh-N-conditioned medium (Hh). Lanes 3–7: cells transfected with *ptc* double-strand RNA and allowed to recover after transfection for the indicated times before harvesting. Lanes 8–12: cells transfected with *mastermind* double-strand RNA as a control. Ptc levels decreased to a minimum by 32 hr and remained essentially constant thereafter. Smo shifts to the slow migrating form and accumulates between 20 and 32 hr. Transfection is unlikely to affect every cell. The low level of Ptc remaining after 32 hr may reflect expression in untransfected cells. This was estimated to be less than 5% based on quantitation of a shorter exposure of the blot. Ptc and Smo levels were unaffected by control dsRNA.

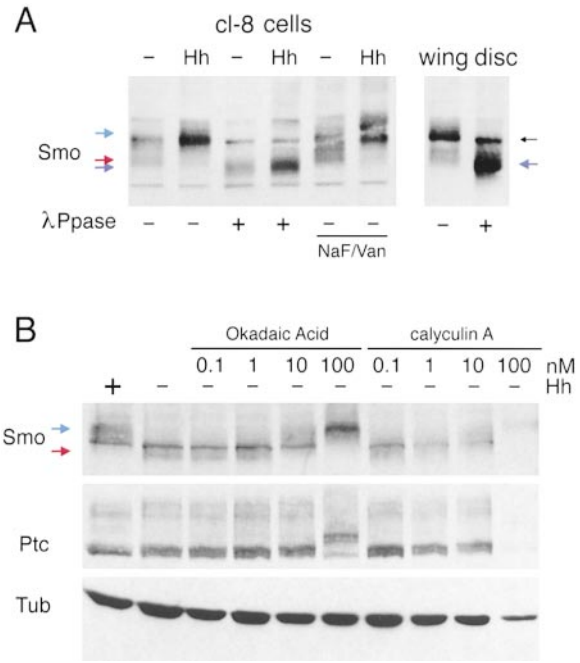


Figure 7. Hh Regulates Smo Phosphorylation

(A) Immunoblot of clone 8 cell and wing imaginal disc lysates probed with anti-Smo. cl-8 cells were treated for 2 hr with S2 (−) or Hh-conditioned medium (Hh). Lysates were prepared and incubated with (+) or without (−) lambda phosphatase. Wing disc lysates were incubated with or without added phosphatase. Red and blue arrows are as in Figure 5. The purple arrow indicates a faster migrating form of Smo generated by phosphatase treatment. We noted that some dephosphorylation occurs during incubation of the control cell lysates without added phosphatase. Addition of the phosphatase inhibitors sodium fluoride and sodium orthovanadate to the control incubation mixture revealed a more extensive mobility shift in Hh-treated cells and appeared to stabilize the faster mobility forms of Smo in control cell lysates. Wing disc and cl-8 cell lysates were run on the same gel (intervening lanes are not shown).

(B) Immunoblot of clone 8 cells treated for 2 hr with Hh-conditioned medium or with S2 (−) conditioned medium and the indicated concentrations of okadaic acid or calyculin A. The blot was probed with anti-Smo, reprobed with anti-Ptc, and then with anti-tubulin as a loading control. Smo mobility shifts between 1 and 10 nM okadaic acid and calyculin A. Calyculin A appeared to cause damage to cells at higher concentrations and reduced the recovery of total cell protein.

chains decreased the apparent size of Smo from both Hh-stimulated and unstimulated cells but did not eliminate the Hh-induced difference in Smo mobility (data not shown). Dephosphorylation of cl-8 cell lysates with lambda phosphatase eliminated the mobility difference in Smo from Hh-stimulated cells and control cells (Figure 7A, purple arrow). In both cases, dephosphorylation produced a new faster-migrating form of Smo. Dephosphorylation of wing disc lysates produced a similar shift to the fastest migrating form. These observations suggest that Smo is phosphorylated to some extent in unstimulated cl-8 cells and that Hh treatment increases the amount of phosphorylation or alters the type of phosphorylation to induce a further shift in electrophoretic mobility. In the wing disc, most of the Smo protein exists in the highly phosphorylated form and a small proportion exists in the less phosphorylated form corresponding to that seen in unstimulated cl-8 cells. The less phosphorylated form may reflect the state of Smo protein in anterior compartment cells that are not exposed to Hh in the wing disc (Figure 1A).

Treatment of cl-8 cells with the phosphatase inhibitors okadaic acid or calyculin A produced shifts in the mobility of Smo similar to that induced by Hh treatment (Figure 7B). Both inhibitors showed dose-dependent effects between 1 and 10 nM. At 100 nM, okadaic acid caused a more complete shift in Smo mobility toward the slowest migrating form and also affected mobility of Ptc. We noted that the amount of Smo protein increased in cells treated with 100 nM okadaic acid, although levels of total cell protein were unaffected. This observation suggests that the state of Smo phosphorylation might influence the relative stability of Smo protein in cells. As noted above, the slower migrating, phosphorylated form of Smo appears to be more stable than the less phosphorylated form in the absence of new protein synthesis (Figure 5C).

## Distinct Subcellular Localization of Ptc and Smo in Hh-Stimulated Cells

Immunoprecipitation studies on epitope-tagged vertebrate Ptc and Smo proteins expressed in transfected cells have suggested that Ptc and Smo exist in a preformed complex that is activated by Sonic Hh binding (Stone et al., 1996). We were therefore surprised to observe that Hh treatment had opposing effects on Ptc and Smo proteins in cycloheximide-treated cells (Figure 5). Hh-induced accumulation of the slower-migrating phosphorylated form of Smo was found to correlate with a reduction in the level of Ptc protein. Ptc levels were reduced in both cl-8 and S2 cells treated with Hh and cycloheximide compared to cells treated with cycloheximide alone (Figures 5B and 5C; compare Ptc levels to “ns” or tubulin in lanes 3, 4 and 7, 8). In S2 cells, which lack Ci and should not be able to induce new Ptc synthesis in response to Hh, Hh treatment was sufficient to

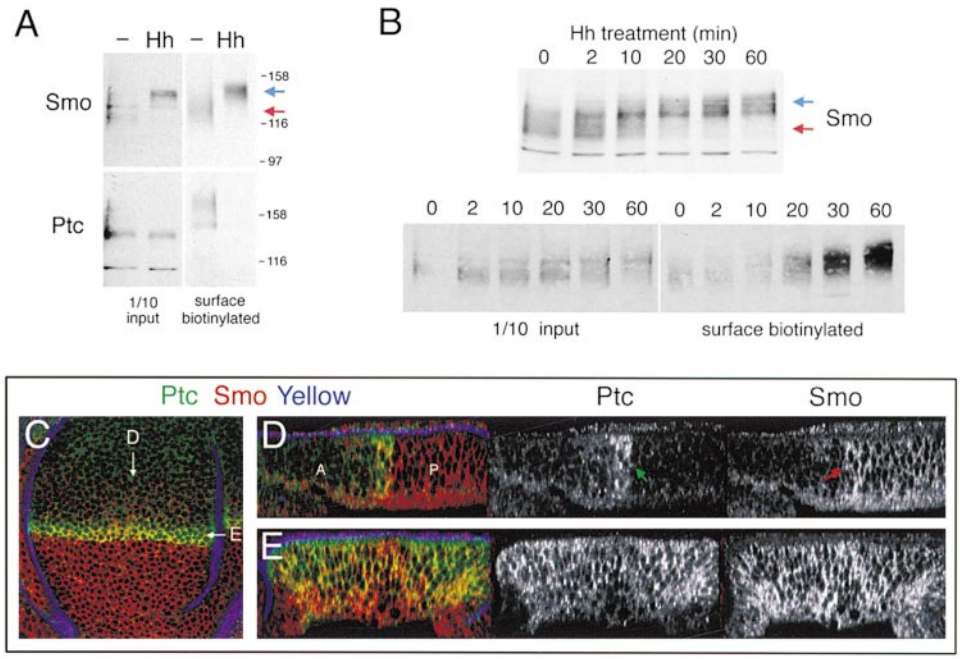


Figure 8. Subcellular Distribution of Ptc and Smo

(A) Cell surface proteins were labeled by surface biotinylation of cl-8 cells. Left panels show immunoblots of 1/10 of the input of the surface-biotinylated cell lysate. Right panels show the biotin-labeled proteins recovered by avidin-mediated affinity purification.

(B) Time course of Smo modification by Hh. Cells were treated with Hh-conditioned medium for the indicated times. Upper panel: whole-cell lysates were prepared and analyzed by immunoblotting with anti-Smo. Lower panel: left, 1/10 of the input of the surface-biotinylated cell lysate; right, surface-biotinylated Smo recovered by avidin-mediated affinity purification.

(C–E) Wing discs labeled to visualize Ptc (green), Smo (red), and Yellow (blue) proteins. Yellow protein marks the apical side of the epithelium.

(C) Horizontal optical section.

(D) Optical cross section of another disc along the AP axis (approximately as indicated by the arrow in [C]). This section allows comparison of the subcellular localization of Smo and Ptc in P cells, A cells, and in Hh-responsive cells adjacent to the AP boundary.

(E) Optical cross section of the disc in (C) along the plane indicated by the arrow labeled (E). This section is shown to provide an extended view of AP boundary cells that are receiving the Hh signal. Smo is not concentrated in the Ptc-containing vesicles. In many cases, there is no detectable Smo in these vesicles.

reduce Ptc levels (Figure 5B, compare lanes 1, 2 and 5, 6). These observations suggest that Hh induces turnover of Ptc. Turnover of Ptc can be observed when new synthesis is not permitted but is masked in normal cells.

This observation prompted us to look more closely at the effect of Hh on the relationship between Ptc and Smo at the cell surface. Cl-8 cells were treated with Hh or with control S2 medium for 60 min, and cell surface proteins were labeled by biotinylation. Hh treatment had strikingly opposite effects on the accessibility of Ptc and Smo to biotinylation. In untreated cells, a fraction of Ptc protein was accessible for surface biotinylation (Figure 8A, lower panels). In Hh-treated cells, the level of cell surface Ptc was reduced considerably, although the total level of Ptc in the cl-8 cell lysates was unchanged. In contrast, Hh treatment increased the level of Smo on the cell surface (Figure 8A, upper panel). In whole-cell lysates the shift of Smo to the slower migrating, phosphorylated form occurred gradually between 10 and 30 min after addition of Hh-conditioned medium (Figure 8B, upper panel). The increase in surface-biotinylated Smo was evident by 20 min and continued to increase through 60 min of Hh treatment (Figure 8B, lower panel). During the short time course of this experiment, there was little net accumulation of Smo, yet there was a marked change in the proportion of Smo accessible to biotinylation at the cell surface. These observations suggest that Hh treatment leads to internalization of Ptc from the cell surface while concomitantly leading to an increase in level of Smo accessible on the cell surface. This could reflect a redistribution of Smo from an intracellular pool to the cell surface or could reflect altered stability or accessibility of cell surface Smo due to removal of Ptc (see also Figure 6). These observations are difficult to reconcile with the idea that Ptc and Smo form a stable receptor complex in vivo.

Double labeling of wing discs supports the observation made in cl-8 cells that Ptc protein is internalized and thus separates from Smo protein in response to Hh stimulation (Figures 8C–8E). Ptc labeling is most intense in intracellular vesicles in Hh-responsive cells. As reported previously, some of these vesicles contain Hh protein (Burke et al., 1999). However, they do not contain elevated levels of Smo (Figures 8D and 8E). On close examination, many Ptc-containing vesicles do not appear to contain detectable levels of Smo protein. Smo protein is mainly observed along the basolateral surface of the cells. Hh-responsive cells show increased accumulation of Smo on the basolateral surface (Figure 8D, red arrow) as well as elevated levels of Ptc (Figure 8D, green arrow). Aside from the Ptc-containing vesicles, it appears that the subcellular localization of the two proteins are at least partly distinct because the regions where Smo labeling is more intense do not correlate with the relative intensity of Ptc labeling (Figure 8E). We

also note that Ptc extends more apically along the lateral membrane than Smo, suggesting that Smo may be limited to a more basolateral domain (Figure 8E).

The observations on the differential effect of Hh on Ptc and Smo in cl-8 cells and in the wing disc suggest that Hh induces a redistribution of Ptc and Smo proteins to distinct domains within the cell. Hh treatment appears to cause internalization of Ptc and an increase in Smo at the cell surface. Hh treatment prevents a Patched-dependent alteration in posttranslational modification of Smo.

## Discussion

Patched and Smoothened proteins play distinct roles in transduction of the Hh signal. Ptc is required for Hh binding, whereas Smo is required to transduce the signal (Alcedo et al., 1996; Chen and Struhl, 1996, 1998; Marigo et al., 1996; Stone et al., 1996; van den Heuvel and Ingham, 1996; Murone et al., 1999). Ptc blocks the intrinsic signaling activity of Smo, and Hh binding to Ptc alleviates this block and thereby activates Smo. The available evidence suggests that Hh does not bind to Smo in the absence of Ptc (Stone et al., 1996) nor does Hh activity appear to be required to activate Smo in the absence of Ptc (as suggested by the effects of far anterior *ptc* mutant clones in the wing disc). This has raised the possibility that Smo might be constitutively active when the inhibitory effects of Ptc are alleviated. These observations have led to a model in which Ptc and Smo exist in a preformed complex at the cell surface that is activated by Hh binding. Three observations from our analysis support an alternative view of the relationship between Smo and Ptc in Hh signaling: (1) Ptc acts to reduce the level of Smo protein in the absence of Hh. (2) Hh binding triggers removal of Ptc from the cell surface. (3) Hh treatment or removal of Ptc by RNA(i) induces a net increase in phosphorylation of Smo. This correlates with an increase in the level of Smo on the cell surface. These observations raise the possibility that Ptc acts indirectly to regulate Smo activity.

### Hh-Dependent Modification of Smoothened

How does Hh treatment alter the degree of Smo phosphorylation? Hh binding to Ptc could stimulate the activity of a kinase that phosphorylates Smo. Alternatively, the constitutive activity of Ptc could be mediated by promoting dephosphorylation of Smo. If this is the case, Hh treatment might inactivate a Ptc-dependent phosphatase. We favor the second possibility because dsRNA-mediated depletion of Ptc was sufficient to increase Smo phosphorylation in S2 cells without addition of Hh. In the wing disc, most of the Smo protein comes from the posterior compartment where Ptc is not expressed. Smo from the disc is mostly in the highly phosphorylated form. Thus, in the absence of Ptc, Smo is mainly found in the highly phosphorylated form. The available evidence indicates that Smo is active in the P compartment, but the signal is nonproductive due to the absence of Ci (Dominguez et al., 1996; Méthot and Basler, 1999). Taken together, these observations suggest that the highly phosphorylated form of Smo is active in signaling. We suggest that Ptc activity is mediated by promoting dephosphorylation of Smo and that Hh blocks the ability of Ptc regulate Smo in A cells near the AP boundary. The relatively low amount of dephosphorylated Smo seen in discs may derive from anterior cells in which Ptc is active because they are out of the range of Hh.

Our findings are consistent with the possibility that Smo is dephosphorylated by a type 2A protein phosphatase. At the concentrations used in our experiments, okadaic acid inhibits PP2A but not PP1-type phosphatases. Smo protein contains consensus sites for phosphorylation by serine/threonine protein kinases, including PKA (Alcedo et al., 1996; van den Heuvel and Ingham, 1996). The serine/threonine kinase Fused is phosphorylated in response to Hh (Therond et al., 1996) and plays a role in Hh signaling (Alves et al., 1998; Monnier et al., 1998; Therond et al., 1999). In addition, previous work has also implicated PKA and an okadaic acid–sensitive phosphatase in the regulation of Ci phosphorylation (Wang and Holmgren, 1999). Thus, there appear to be several levels at which phosphorylation and dephosphorylation can regulate Hh signaling activity. We favor the model that the constitutive activity of Ptc stimulates activity of a phosphatase that leads to reduced phosphorylation of Smo. Hh binding to Ptc might reduce the ability of Ptc to promote phosphatase activity and allow Smo phosphorylation to increase. According to this view, the state of Smo phosphorylation reflects a balance in the activity of a kinase (which could be constitutively active) and the Ptc-dependent activity of a phosphatase.

### Direct versus Indirect Regulation of Smo by Ptc

We have presented evidence that Hh induces distinct alterations in the subcellular localization of Ptc and Smo proteins. In cells, Hh treatment induces internalization of Ptc and accumulation of Smo at the cell surface. Double labeling studies have shown that Ptc and Hh colocalize in vesicles in the wing disc (Burke et al., 1999). In embryos, immunoelectronmicroscopic analysis has shown that Ptc is found in endocytic vesicles and in multivesicular bodies (Capdevila et al., 1994). Multivesicular bodies are intermediates between early and late endosome compartments. The appearance of Ptc in multivesicular bodies is consistent with the possibility that Hh-induced endocytosis targets Ptc to the lysosome for degradation. In this context, it is interesting that Ptc shows sequence similarity to the Niemann-Pick C1 protein, which has been linked to defects in recycling of vesicles in the endocytic and lysosomal pathways (Neufeld et al., 1999; Incardona and Eaton, 2000). Together, these observations support the view that Hh binding triggers internalization and degradation of Ptc. Under normal circumstances, Hh signaling induces new synthesis of Ptc, which serves to limit the range of Hh movement into the A compartment (Chen and Struhl, 1996). These apparently opposing effects on Ptc levels may be reconciled by the idea that this mechanism is used to target Hh for degradation once it has bound Ptc and activated Smo. Clearing Hh from the system may contribute to limiting its range of movement.

Smo does not appear to follow Ptc through the endocytic pathway. In contrast, Smo accumulates on the cell surface in Hh-stimulated cells. Accumulation of Smo could reflect Hh-induced transport of Smo from an intracellular pool to the cell surface. Alternatively, Hh-induced phosphorylation might reduce Smo turnover in the membrane, leading to net accumulation. At present, we cannot distinguish between these possibilities.

Whatever the mechanism for increased accumulation of Smo at the cell surface, our observations suggest that the actively signaling form of Smo is unlikely to be bound by Ptc. If Ptc acts indirectly to regulate Smo activity, the regulatory interaction between Ptc and Smo need not be stoichiometric. We note that levels of Smo protein significantly in excess of normal can be rendered functionally inactive by endogenous levels of Ptc (Figure 2). Although it is possible to exceed the capacity of Ptc to regulate Smo activity by overexpression (for example, Figure 2G), our results illustrate that Ptc can effectively regulate both Smo activity and Smo protein levels over a considerable range and at levels well above the endogenous level of Smo. These observations support the possibility that Ptc might act indirectly to regulate Smo phosphorylation, with concomitant effects on subcellular localization, stability, and activity.

## Experimental Procedures

### *Drosophila* Strains

Mutant and transgenic strains are described in the following references: *smo*$^{3}$ (Chen and Struhl, 1998); *ptc*$^{llw}$, *ptc*$^{6P}$ (Capdevila et al., 1994); *hh*$^{ts2}$ (Ma et al., 1993); *pka-C1*$^{H2}$ (Li et al., 1995); *EP(2)0941*$^{ptc}$ (Rorth et al., 1998); *apterous*$^{Gal4}$ (Calleja et al., 1996); *Act5C>CD2>Gal4* (Pignoni and Zipursky, 1997); *UAS-Hh* (Ingham, 1995); and *UAS-Hh-CD2* (Strigini and Cohen, 1997).

*UAS-EGFP* was prepared by Maura Strigini (http://flybase.bio.indiana.edu:82/.bin/fbidq.html?FBrf0112155). *UAS-Smo*: Smo cDNA (Alcedo et al., 1996) was digested with NotI and XhoI and cloned into pUAST. *UAS-Smo-TAP*: a portion of the Smo coding sequence was amplified by PCR to introduce a BspHI site in place of the stop codon (5′-TTTCATACTAGTGGCCATTGCGTGCC and the 3′-TTTTTCATGACCCCTTTTGAAGGCAGCAATAAC). The PCR product was digested with SpeI and BspHI and ligated with an NcoI–XbaI fragment containing the TAP epitope tag (Rigaut et al., 1999) in a three-part ligation with SpeI–XbaI digested pUAST-Smo as the vector. The resulting fusion protein consists of a TAP tag added to the C terminus of Smo.

### Genotypes of Larvae for Generating Mosaic Clones

#### *Flip-Out Clones*

Smo: Act5C>CD2>Gal4/HSFlp1; UAS-EGFP/UAS-Smo
Hh: Act5C>CD2>Gal4/HSFlp1; UAS-EGFP/+; UAS-hh/+
HhCD2: Act5C>CD2>Gal4/HSFlp1; UAS-EGFP/+; UAS-hhCD2/+
Ptc in hh$^{ts2}$ mutant background: Act5C>CD2>Gal4/HSFlp1; EP(2)0941$^{ptc}$/+; hh$^{ts2}$

#### *Mutant Clones*

smo: HSFlp1; smo$^{3}$ FRT40A/armadillo-lacZ FRT40A
ptc: HSFlp1; FRT43D ptc$^{6P}$/FRT43D armadillo-lacZ and HSFlp1; FRT42 ptc$^{llW}$/FRT42 armadillo-lacZ

### Antibodies

Rabbit anti-Ci (Schwartz et al., 1995); rat monoclonal anti-Ci (2A1; Motzny and Holmgren, 1995); anti-Ptc (Capdevila et al., 1994) and monoclonal 5D10 (kindly provided by Phil Ingham); mouse monoclonal anti-En 4D9 (Patel et al., 1989); rabbit anti-Yellow (Kornezos and Chia, 1992); and mouse anti-tubulin (Sigma), rabbit peroxidase anti-peroxidase (Sigma) was used to detect the protein A moiety in the TAP tag. In control experiments, the TAP tag showed no detectable binding of rat or mouse primary antibodies or of goat and donkey secondary antibodies.

### Production of Smoothened Antibody

A fragment of Smo from nucleotide 1692 to nucleotide 3348 was amplified by PCR (5′ primer TTTCATACTAGTGGCCATTGCGTGCC; 3′ primer TTTTTCTCGAGTTTTGAAGGCAGCAATAAC) and cloned into pCRscript (Stratagene). The resulting plasmid was digested with MunI and XhoI, and the fragment was cloned into EcoRI- and XhoI-digested pET23c (Novagen). The resulting fusion protein consisted of amino acids (aa) 560–1036 of Smo with a C-terminal His tag. The bacterially expressed fusion protein was recovered as an insoluble pellet. The pellet was solubilized in 8 M urea, 0.1 M $NaH_2PO_4$, and 0.01 M Tris-HCl (pH 8) and purified on a $Ni^{2+}$ column under denaturing conditions. Rats were immunized with 50 μg of purified fusion protein in RIBI adjuvant at intervals of 3 weeks.

### Cell Culture and Drug Treatment

cl-8 cells were cultured as described in van Leeuwen et al. (1994). As the Hh-N-producing cell line obtained from other sources was nonfunctional, a new cell line was prepared as follows: a fragment encoding aa residues 1–257 of Hh was amplified by PCR (5′ primer: AGAGAATTCATGGATAACCACAGC; 3′ primer: TTTGGTACCTTAG CCGTGCACGTGGGA) and cloned into pRmHa3. A puromycin resistance marker was introduced as an MluI fragment into the unique AatI site of pRmHa3 (converted to MluI by insertion of an oligonucleotide). Stable cell lines were selected in puromycin following transfection. Conditioned medium was collected from cells induced with 0.7 mM CuSO4 in S2 medium without puromycin for 24 hr. Cells were plated in 6-well plates and treated with Hh-N or control S2-conditioned medium for the indicated times. Cells were washed twice with PBS-containing protease inhibitors (Complete, Boehringer, supplemented with 1 mM PMSF) and lysed by addition of 6× SDS–PAGE sample buffer. For Figure 4, cycloheximide was added to a final concentration of 10 μM. For Figure 7, cells were treated for 2 hr with the phosphatase inhibitors okadaic acid and calyculin A at the indicated concentrations. Cells were lysed in 50 mM Tris (pH 8), 150 mM NaCl, 2% NP40 containing 25 mM NaF, 400 μM sodium orthovanadate, and protease inhibitors. For lambda phosphatase treatment, cells were lysed by incubation for 15 min on ice in 50 mM Tris (pH 8), 150 mM NaCl, and 2% NP40 containing protease inhibitors. Discs were ground in the same buffer in a dounce homogenizer. Lysates were cleared by centrifugation and incubated with ~200 U of lambda phosphatase for 30 min at 30°C in 50 mM Tris (pH 8), 150 mM NaCl, 2% NP40 adjusted to 2 mM $MnCl_2$, 0.1 mM NaEDTA, 5 mM DTT, and 0.1% Brij 35. Digestion was stopped by addition of SDS–PAGE sample buffer.

### RNA Interference in S2 Cells

Double-stranded RNA was produced by in vitro transcription using T7 polymerase on PCR products corresponding to residues 3301–4064 and 3828–4690 of *ptc* mRNA (X17558) or on a cloned fragment corresponding to residues 1278–1471 of *mastermind* (X54251). PCR primers included the T7 promoter. Both fragments of *ptc* were equally effective. S2 cells were transfected with 12 μg of dsRNA in 600 μl using lipofectin. After 8 hr, the transfection mix was removed and cells were cultured in S2-conditioned medium (without Hh). Samples were processed for SDS–PAGE and immunoblotting as above.

### Cell Surface Biotinylation

Cells were incubated for the indicated times in Hh-conditioned or S2-conditioned medium, washed with ice-cold PBS, and incubated for 20 min in ice-cold PBS containing 1 mg/ml Sulfo-NHS-LC-Biotin (Pierce). Biotinylation was quenched by incubating cells with ice-cold PBS containing 100 mM glycine for 25 min. Cells were washed in PBS and lysed in PBS containing 2% NP40, 0.2% SDS, 25 mM NaF, 400 μM sodium orthovanadate, and protease inhibitors. The lysate was clarified by centrifugation, and biotinylated proteins were recovered by binding to streptavidin-agarose beads (Pierce) overnight at 4°C. Beads were washed and proteins recovered in SDS–PAGE sample buffer.

### Acknowledgments

We thank Ann-Mari Voie for preparing transgenic fly strains; Phil Ingham and Isabel Guerrero for anti-Ptc; Suzanne Eaton for anti-Yellow; Tom Kornberg, Carol Schwartz, and Bob Holmgren for anti-Ci and fly strains; and Angel Nebreda for providing phosphatases, inhibitors, and advice. We thank Pernilly Rørth for discussions. N. D. was supported by a fellowship from the Fonds Voor Wetenschappelijk Onderzoek-Vlaanderen.

Received April 18, 2000; revised June 5, 2000.

**References**

Alcedo, J., and Noll, M. (1997). Hedgehog and its Patched-Smoothened receptor complex: a novel signaling mechanism at the cell surface. Biol. Chem. *378*, 583–590.

Alcedo, J., Ayzenzon, M., von Ohlen, T., Noll, M., and Hooper, J. (1996). The Drosophila *smoothened* gene encodes a seven-pass membrane protein, a putative receptor for the Hedgehog signal. Cell *86*, 221–232.

Alexandre, C., Jacinto, A., and Ingham, P.W. (1996). Transcriptional activation of hedgehog target genes in Drosophila is mediated directly by the cubitus interruptus protein, a member of the GLI family of zinc finger DNA-binding proteins. Genes Dev. *10*, 2003–2013.

Alves, G., Limbourg-Bouchon, B., Tricoire, H., Brissard-Zahraoui, J., Lamour-Isnard, C., and Busson, D. (1998). Modulation of Hedgehog target gene expression by the Fused serine-threonine kinase in wing imaginal discs. Mech. Dev. *78*, 17–31.

Aza-Blanc, P., and Kornberg, T.B. (1999). Ci, a complex transducer of the Hedgehog signal. Trends Genet. *15*, 458–462.

Aza-Blanc, P., Ramírez-Weber, F.-A., Laget, M.-P., Schwartz, C., and Kornberg, T.B. (1997). Proteolysis that is inhibited by Hedgehog targets Cubitus interruptus protein to the nucleus and converts it to a repressor. Cell *89*, 1043–1053.

Basler, K., and Struhl, G. (1994). Compartment boundaries and the control of *Drosophila* limb pattern by *hedgehog* protein. Nature *368*, 208–214.

Brook, W.J., and Cohen, S.M. (1996). Antagonistic interactions between Wingless and Decapentaplegic responsible for dorsal-ventral pattern in the Drosophila leg. Science *273*, 1373–1377.

Burke, R., Nellen, D., Bellotto, M., Hafen, E., Senti, K.A., Dickson, B.J., and Basler, K. (1999). Dispatched, a novel sterol-sensing domain protein dedicated to the release of cholesterol-modified hedgehog from signaling cells. Cell *99*, 803–815.

Calleja, M., Moreno, E., Pelaz, S., and Morata, G. (1996). Visualization of gene expression in living adult Drosophila. Science *274*, 252–255.

Capdevila, J., Estrada, M.P., Sánchez-Herrero, E., and Guerrero, I. (1994). The *Drosophila* segment polarity gene *patched* interacts with *decapentaplegic* in wing development. EMBO J. *13*, 71–82.

Chen, Y., and Struhl, G. (1996). Dual roles for Patched in sequestering and transducing Hedgehog. Cell *87*, 553–563.

Chen, Y., and Struhl, G. (1998). In vivo evidence that Patched and Smoothened constitute distinct binding and transducing components of a Hedgehog receptor complex. Development *125*, 4943–4948.

Chen, C.-H., von Kessler, D.P., Park, W., Wang, B., Ma, Y., and Beachy, P.A. (1999). Nuclear trafficking of Cubitus interruptus in the transcriptional regulation of Hedgehog target gene expression. Cell *98*, 305–316.

Diaz-Benjumea, F.J., Cohen, B., and Cohen, S.M. (1994). Cell interactions between compartments establishes the proximal-distal axis of *Drosophila* limbs. Nature *372*, 175–179.

Dominguez, M., Brunner, M., Hafen, E., and Basler, K. (1996). Sending and receiving the Hedgehog signal: control by the *Drosophila* Gli protein Cubitus interruptus. Science *272*, 1621–1625.

Hammond, S.M., Bernstein, E., Beach, D., and Hannon, G.J. (2000). An RNA-directed nuclease mediates post-transcriptional gene silencing in Drosophila cells. Nature *404*, 293–296.

Hepker, J., Wang, Q.-T., Motzny, C.K., Holmgren, R., and Orenic, T.V. (1997). Drosophila *cubitus interruptus* forms a negative feedback loop with Patched and regulates expression of Hedgehog target genes. Development *124*, 549–558.

Incardona, J.P., and Eaton, S. (2000). Cholesterol in signal transduction. Curr. Opin. Cell Biol. *12*, 193–203.

Ingham, P.W. (1995). Signaling by Hedgehog family proteins in *Drosophila* and vertebrate development. Curr. Opin. Genet. Dev. *5*, 492–498.

Ingham, P.W., Taylor, A.M., and Nakano, Y. (1991). Role of the *Drosophila patched* gene in positional signalling. Nature *353*, 184–187.

Jiang, J., and Struhl, G. (1996). Complementary and mutually exclusive activities of Decapentaplegic and Wingless organize axial pattern during Drosophila limb development. Cell *86*, 401–409.

Kornezos, A., and Chia, W. (1992). Apical secretion and association of the Drosophila yellow gene product with developing larval cuticle structures during embryogenesis. Mol. Gen. Genet. *235*, 397–405.

Lecuit, T., and Cohen, S.M. (1997). Proximal-distal axis formation in the Drosophila leg. Nature *388*, 139–145.

Lecuit, T., Brook, W.J., Ng, M., Calleja, M., Sun, H., and Cohen, S.M. (1996). Two distinct mechanisms for long-range patterning by Decapentaplegic in the Drosophila wing. Nature *381*, 387–393.

Lee, J.J., von Kessler, D.P., Parks, S., and Beachy, P.A. (1992). Secretion and localized transcript suggest a role in positional signalling for products of the segmentation gene *hedgehog*. Cell *71*, 33–50.

Li, W., Ohlmeyer, J.T., Lane, M.E., and Kalderon, D. (1995). Function of protein kinase A in Hedgehog signal transduction and Drosophila imaginal disc development. Cell *80*, 553–562.

Ma, C., Zhou, Y., Beachy, P., and Moses, K. (1993). The segment polarity gene *hedgehog* is required for progression of the morphogenetic furrow in the developing Drosophila eye. Cell *75*, 927–938.

Marigo, V., Davey, R.A., Zuo, Y., Cunnigham, J.M., and Tabin, C.J. (1996). Biochemical evidence that Patched is the Hedgehog receptor. Nature *384*, 176–179.

Méthot, N., and Basler, K. (1999). Hedgehog controls limb development by regulating the activities of distinct transcriptional activator and repressor forms of Cubitus interruptus. Cell *96*, 819–831.

Monnier, V., Dussillol, F., Alves, G., Lamour-Isnard, C., and Plessis, A. (1998). Suppressor of fused links fused and Cubitus interruptus on the hedgehog signalling pathway. Curr. Biol. *8*, 583–586.

Motzny, C.K., and Holmgren, R.A. (1995). The *Drosophila* cubitus interruptus protein and its role in *wingless* and *hedgehog* signal transduction pathways. Mech. Dev. *52*, 137–150.

Mullor, J.L., Calleja, M., Capdevila, J., and Guerrero, I. (1997). Hedgehog activity, independent of Decapentaplegic, participates in wing disc patterning. Development *124*, 1227–1237.

Murone, M.A.R., and de Sauvage, F.J. (1999). Sonic hedgehog signaling by the Patched-Smoothened receptor complex. Curr. Biol. *9*, 76–84.

Nellen, D., Burke, R., Struhl, G., and Basler, K. (1996). Direct and long-range action of a Dpp morphogen gradient. Cell *85*, 357–368.

Neufeld, E.B., Wastney, M., Patel, S., Suresh, S., Cooney, A.M., Dwyer, N.K., Roff, C.F., Ohno, K., Morris, J.A., Carstea, E.D., et al. (1999). The Niemann-Pick C1 protein resides in a vesicular compartment linked to retrograde transport of multiple lysosomal cargo. J. Biol. Chem. *274*, 9627–9635.

Ohlmeyer, J.T., and Kalderon, D. (1998). Hedgehog stimulates maturation of Cubitus interruptus into a labile transcriptional activator. Nature *396*, 749–753.

Patel, N.H., Martin-Blanco, E., Coleman, K.G., Poole, S.J., Ellis, M.C., Kornberg, T.B., and Goodman, C.S. (1989). Expression of *engrailed* proteins in Arthropods, Annelids, and Chordates. Cell *58*, 955–968.

Pignoni, F., and Zipursky, S.L. (1997). Induction of Drosophila eye development by decapentaplegic. Development *124*, 271–278.

Rigaut, G., Shevchenko, A., Rutz, B., Wilm, M., Mann, M., and Séraphin, B. (1999). A generic protein purification method for protein complex characterization and proteome exploration. Nat. Biotechnol. *17*, 1030–1032.

Rorth, P., Szabo, K., Bailey, A., Laverty, T., Rehm, J., Rubin, G.M., Weigmann, K., Milan, M., Benes, V., Ansorge, W., and Cohen, S.M. (1998). Systematic gain-of-function genetics in Drosophila. Development *125*, 1049–1057.

Schwartz, C., Locke, J., Nishida, C., and Kornberg, T.B. (1995). Analysis of *cubitus interruptus* regulation in *Drosophila* embryos and imaginal discs. Development *121*, 1625–1635.

Stone, D.M., Hynes, M., Armanini, M., Swanson, T.A., Gu, Q., Johnson, R.L., Scott, M.P., Pennica, D., Goddard, A., Phillips, H., et al. (1996). The tumor-suppressor gene *patched* encodes a candidate receptor for Sonic hedgehog. Nature *384*, 129–134.

Strigini, M., and Cohen, S.M. (1997). A Hedgehog activity gradient contributes to AP axial patterning of the Drosophila wing. Development *124*, 4697–4705.

Tabata, T., and Kornberg, T. (1994). Hedgehog is a signalling protein with a key role in patterning Drosophila imaginal discs. Cell *76*, 89–102.

Tabata, T., Eaton, S., and Kornberg, T.B. (1992). The *Drosophila hedgehog* gene is expressed specifically in posterior compartment cells and is a target of *engrailed* regulation. Genes Dev. *6*, 2635–2645.

Therond, P.P., Knight, J.D., Kornberg, T.B., and Bishop, J.M. (1996). Phosphorylation of the fused protein kinase in response to signaling from hedgehog. Proc. Natl. Acad. Sci. USA *93*, 4224–4228.

Therond, P.P., Limbourg Bouchon, B., Gallet, A., Dussilol, F., Pietri, T., van den Heuvel, M., and Tricoire, H. (1999). Differential requirements of the fused kinase for hedgehog signalling in the Drosophila embryo. Development *126*, 4039–4051.

van den Heuvel, M., and Ingham, P.W. (1996). *smoothened* encodes a receptor-like serpentine protein required for *Hedgehog* signaling. Nature *382*, 547–551.

van Leeuwen, F., Harryman Samos, C., and Nusse, R. (1994). Biological activity of soluble *wingless* protein in *Drosophila* imaginal disc cells. Nature *368*, 342–344.

Wang, Q.T., and Holmgren, R.A. (1999). The subcellular localization and activity of *Drosophila* Cubitus interruptus are regulated at multiple levels. Development *126*, 5097–5106.

Zecca, M., Basler, K., and Struhl, G. (1995). Sequential organizing activities of *engrailed, hedgehog* and *decapentaplegic* in the Drosophila wing. Development *121*, 2265–2278.

**Note Added in Proof**

Alcedo et al. in this month's issue of *Molecular Cell* (Posttranscriptional Regulation of Smoothened Is Part of a Self-Correcting Mechanism in the Hedgehog Signaling System, Mol. Cell *6* (2), 2000) present an independent line of evidence for posttranscriptional regulation of Smoothened protein levels in embryonic development.